

ITERATIVE MMSE DETECTION FOR MIMO/BLAST DS-CDMA SYSTEMS IN FREQUENCY SELECTIVE FADING CHANNELS

Achieving High Performance in Fully Loaded Systems

João Carlos Silva, Nuno Souto, Francisco Cercas

Instituto Superior Técnico/IT, Torre Norte 11-11, Av. Rovisco Pais 1, 1049-001 Lisboa, Portugal

Rui Dinis

CAPS, Av. Rovisco Pais 1, 1049-001 Lisboa, Portugal

Keywords: MIMO-BLAST, Iterative Interference Canceller, W-CDMA.

Abstract: A MMSE (Minimum Mean Square Error) DS-CDMA (Direct Sequence-Code Division Multiple Access) receiver coupled with a low-complexity iterative interference suppression algorithm was devised for a MIMO/BLAST (Multiple Input, Multiple Output / Bell Laboratories Layered Space Time) system in order to improve system performance, considering frequency selective fading channels. The scheme is compared against the simple MMSE receiver, for both QPSK and 16QAM modulations, under SISO (Single Input, Single Output) and MIMO systems, the latter with 2Tx by 2Rx and 4Tx by 4Rx (MIMO order 2 and 4 respectively) antennas. To assess its performance in an existing system, the uncoded UMTS HSDPA (High Speed Downlink Packet Access) standard was considered.

1 INTRODUCTION

MIMO systems have been considered to be one of the most significant technical breakthroughs in modern communications, since they can augment significantly the system capacity, by increasing the number of both transmit and receive antennas (Foschini, 1998). Just a few years after its invention the technology is already part of the standards for wireless local area networks (WLAN), third-generation (3G) networks and beyond.

The receiver for such a scheme is obviously complex; due to the number of antennas, users and multipath components, the performance of a simple RAKE/ MF (Matched Filter) receiver (or enhanced schemes based on the MF) has a severe interference canceling limitation, that does not allow for the system to perform at full capacity. Therefore, a MMSE receiver (Latva-aho, 2000), adapted for multipath MIMO, was developed for such cases acting as an equalizer, yielding interesting results. In order to further augment the MMSE receiver's performance, an additional low complexity block performing interference suppression was added.

Although the MMSE guarantees the minimum variance estimates, some estimates may exceed the threshold value in which they are supposed to be. The interference suppression block has a built-in SDD (Soft Decision Device), so that the initial estimates are adjusted in order to minimize their mean square error. The new estimates are then introduced in a iterative Parallel Interference Canceller (PIC) based solely on low complexity matched-filtering, so that a new solution is found within the imposed constraints. Such a scheme produces a performance improvement with little added complexity, when compared to the simple MMSE decoder.

The structure of the paper is as follows. In Section II, the MMSE receiver for MIMO with multipath is introduced. The simulation setup is detailed and results are discussed in Section III. The main conclusions are drawn in Section IV.

2 MMSE RECEIVER

A standard model for a DS-CDMA system with K users (assuming 1 user per physical channel) and L propagation paths is considered. The modulated symbols are spread by a Walsh-Hadamard code with length equal to the Spreading Factor (SF). The signal on a MIMO-BLAST system with N_{TX} transmit and N_{RX} receive antennas, at one of the receiver's antennas, can be expressed as:

$$r_v(t)_{RX=1} = \sum_{n=1}^N \sum_{tx=1}^{N_{TX}} \sum_{k=1}^K \mathbf{A}_{k,tx} \mathbf{b}_{k,tx}^{(n)} \mathbf{c}_{k,tx,rx}(t) s_k(t - nT - \tau_{k,l}) + \mathbf{n}(t)$$

where N is the number of received symbols, $\mathbf{A}_{k,tx} = \sqrt{E_k}$, E_k is the energy per symbol, K is the

number of users, $\mathbf{b}_{k,tx}^{(n)}$ is the n -th transmitted data symbol of user k and transmit antenna tx , $s_k(t)$ is the k -th user's signature signal (equal for all antennas), T denotes the symbol interval, $\mathbf{n}(t)$ is a complex zero-mean AWGN (Additive White Gaussian Noise) with variance σ^2 , $\mathbf{c}_{k,tx,rx}(t) = \sum_{l=1}^L \mathbf{c}_{k,tx,rx,l}^{(n)} \delta(t - \tau_{k,l})$

is the impulse response of the k th user's radio channel, $\mathbf{c}_{k,tx,rx,l}$ is the complex attenuation factor of the k -th user's l -th path of the link between the tx -th and rx -th antenna and $\tau_{k,l}$ is the propagation delay (assumed equal for all antennas).

Using matrix algebra, the received signal can be represented as

$$\mathbf{r}_v = \mathbf{S} \mathbf{C} \mathbf{A} \mathbf{b} + \mathbf{n},$$

where \mathbf{S} , \mathbf{C} and \mathbf{A} are the spreading, channel and amplitude matrices respectively.

The spreading matrix \mathbf{S} has dimensions $(SF \cdot N \cdot N_{RX} + \rho_{MAX} \cdot N_{RX}) \times (K \cdot L \cdot N \cdot N_{TX})$ (ρ_{max} is the maximum delay of the channel's impulse response, normalized to number of chips, and SF is the Spreading Factor), and is composed of sub-matrices \mathbf{S}_{RX} in its diagonal for each receive antenna $\mathbf{S} = \text{diag}(\mathbf{S}_{RX,1}, \mathbf{K}, \mathbf{S}_{RX,N_{RX}})$. Each of these sub-matrices has dimensions $(SF \cdot N + \rho_{MAX}) \times (K \cdot L \cdot N)$, and are further composed by smaller matrices \mathbf{S}_n^L , one for each bit position, with size $(SF + \rho_{MAX}) \times (K \cdot L)$. The \mathbf{S}_{RX} matrix structure is made of $\mathbf{S}_{SRX,n} = [\mathbf{S}_{SRX,1}, \mathbf{K}, \mathbf{S}_{SRX,N}]$, with

$$\mathbf{S}_{SRX,n} = \left[\mathbf{0}_{(SF(n-1) \times (K \cdot L))}; \mathbf{S}_n^L; \mathbf{0}_{(SF(N-n) \times (K \cdot L))} \right]$$

The \mathbf{S}_n^L matrices are made of $K \cdot L$ columns; $\mathbf{S}_n^L = \left[\mathbf{S}_{\text{col}(k=1,l=1),n}, \mathbf{K}, \mathbf{S}_{\text{col}(k=1,l=L),n}, \mathbf{K}, \mathbf{S}_{\text{col}(k=K,l=L),n} \right]$.

Each of these columns is composed of $\mathbf{S}_{\text{col}(kl),n} = \left[\mathbf{0}_{(1 \times \text{delay}(l))}, \mathbf{sp}_n(k)_{1 \times SF}, \mathbf{0}_{(1 \times (\rho_{MAX} - \text{delay}(l)))} \right]^T$, where $\mathbf{sp}_n(k)$ is the combined spreading & scrambling for the bit n of user k .

These \mathbf{S}_n^L matrices are either all alike if no long scrambling code is used, or different if the scrambling sequence is longer than the SF . The \mathbf{S}_n^L matrices represent the combined spreading and scrambling sequences, conjugated with the channel delays. The shifted spreading vectors for the multipath components are all equal to the original sequence of the specific user.

$$\mathbf{S}_n^L = \begin{bmatrix} \mathbf{S}_{1,1,1,n} & \mathbf{L} & \mathbf{L} & \mathbf{S}_{K,1,1,n} \\ \mathbf{M} & \mathbf{O} & \mathbf{S}_{1,1,L,n} & \mathbf{L} & \mathbf{M} & \mathbf{O} & \mathbf{S}_{K,1,L,n} \\ \mathbf{S}_{1,SF,1,n} & & \mathbf{M} & \mathbf{L} & \mathbf{S}_{K,SF,1,n} & & \mathbf{M} \\ & \mathbf{O} & \mathbf{S}_{1,SF,L,n} & \mathbf{L} & \mathbf{L} & \mathbf{O} & \mathbf{S}_{K,SF,L,n} \end{bmatrix}$$

Note that, in order to correctly model the multipath interference between symbols, there is an overlap between the \mathbf{S}_n^L matrices, of ρ_{MAX} .

The channel matrix \mathbf{C} is a $(K \cdot L \cdot N \cdot N_{RX}) \times (K \cdot N_{TX} \cdot N)$ matrix, and is composed of N_{RX} sub-matrices, each one for a receive antenna $\mathbf{C} = [\mathbf{C}_{RX,1}^R; \mathbf{K}; \mathbf{C}_{RX,N_{RX}}^R]$. Each \mathbf{C}^R matrix is composed of N \mathbf{C}^{KT} matrices alongside its diagonals.

$$\mathbf{C} = \begin{bmatrix} \mathbf{C}_{RX,1}^R = \begin{bmatrix} \mathbf{C}_{1,1}^{KT} & & \\ & \mathbf{O} & \\ & & \mathbf{C}_{N,1}^{KT} \end{bmatrix} \\ & & \mathbf{M} \\ \mathbf{C}_{RX,N_{RX}}^R = \begin{bmatrix} \mathbf{C}_{1,N_{RX}}^{KT} & & \\ & \mathbf{O} & \\ & & \mathbf{C}_{N,N_{RX}}^{KT} \end{bmatrix} \end{bmatrix}$$

Each \mathbf{C}^{KT} matrix is $(K \cdot L) \times (K \cdot N_{TX})$, and represents the fading coefficients for the current symbol of each path, user, transmit antenna and receive antenna. The matrix structure is made up of further smaller matrices alongside the diagonal of \mathbf{C}^{KT} , $\mathbf{C}^{KT} = \text{diag}(\mathbf{C}_{K,1}^T, \mathbf{K}, \mathbf{C}_{K,K}^T)$, with \mathbf{C}^T of dimensions $L \times N_{TX}$, representing the fading coefficients for the user's multipath and tx -th antenna component.

$$\mathbf{C}^{KT} = \begin{bmatrix} \mathbf{C}_{1,1,1} & \mathbf{L} & \mathbf{C}_{N_{TX},1,1} \\ \mathbf{M} & & \mathbf{M} \\ \mathbf{C}_{1,1,1} & \mathbf{L} & \mathbf{C}_{N_{TX},1,1} \\ & & \mathbf{O} \\ & & & \mathbf{C}_{1,1,K} & \mathbf{L} & \mathbf{C}_{N_{TX},1,K} \\ & & & \mathbf{M} & & \mathbf{M} \\ & & & \mathbf{C}_{1,1,K} & \mathbf{L} & \mathbf{C}_{N_{TX},1,K} \end{bmatrix}$$

The \mathbf{A} matrix is a diagonal matrix of dimension $(K \cdot N_{TX} \cdot N)$, and represents the amplitude of each user per transmission antenna and symbol, $\mathbf{A} = \text{diag}(\mathbf{A}_{1,1,1,K}, \mathbf{A}_{N_{TX},1,1,K}, \mathbf{A}_{N_{TX},K,1,K}, \mathbf{A}_{N_{TX},K,N})$.

The matrix resultant from the *SCA* operation (henceforth known as *SCA* matrix) is depicted in Figure 1. It is a $N_{TX} \cdot K \cdot N \times N_{RX} \cdot (N \cdot SF + \rho_{MAX})$ matrix, and is the reference matrix for the decoding algorithms.

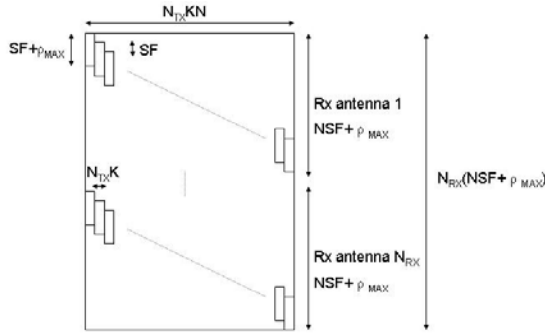


Figure 1 : Layout of the SCA matrix

Vector \mathbf{b} represents the information symbols. It has length $(K \cdot N_{TX} \cdot N)$, and has the following structure $\mathbf{b} = [b_{1,1,1,K}, b_{N_{TX},1,1,K}, b_{1,K,1,K}, b_{N_{TX},K,1,K}, b_{N_{TX},K,N}]^T$. Note that the bits of each transmit antenna are grouped together in the first level, and the bits of other interferers in the second level. This is to guarantee that the resulting matrix to be inverted has all its non-zero values as close to the diagonal as possible. Also note that there is usually a higher correlation between bits from different antennas using the same spreading code, than between bits with different spreading codes.

Finally, the \mathbf{n} vector is a $(N \cdot SF \cdot N_{RX} + N_{RX} \cdot \rho_{MAX})$ vector with noise components to be added to the received vector \mathbf{r}_v , which is partitioned by N_{RX} antennas, $\mathbf{r}_v = [r_{1,1,1,K}, r_{1,SF,1,K}, r_{N,1,1,K}, r_{N,SF+\rho_{MAX},1,K}, r_{N,1,N_{RX}}, r_{N,SF+\rho_{MAX},N_{RX}}]^T$ (note that the delay ρ_{MAX} is only contemplated in the final bit, though its effects are present throughout \mathbf{r}_v).

The MMSE algorithm yields the symbol estimates,

$$\mathbf{y}_{MMSE} = (\mathbf{E}_M)^{-1} \mathbf{y}_{MF}$$

Where \mathbf{y}_{MF} is the (un-normalized) matched filter output

$$\mathbf{y}_{MF} = (\mathbf{SCA})^H \mathbf{r}_v$$

and the \mathbf{E}_M is the Equalization Matrix (cross-correlation matrix of the users' signature sequences after matched filtering, at the receiver)

$$\mathbf{E}_M = \mathbf{R} + \sigma^2 \mathbf{I}$$

with $\mathbf{R} = \times \times^H \times \times^H \times \times \times$ and σ^2 as the noise variance of n .

The configuration is done in such a way that the \mathbf{E}_M presents itself as if the Sparse Reverse Cuthill-McKee ordering algorithm (Liu, 1981) had been applied to it, and thus there is no fill-in when performing the \mathbf{E}_M inverse using the Choleski algorithm. The expected main problem associated with such scheme is the size of the matrices, which assume huge proportions. This has been the main perceived drawback of such scheme, responsible for the reduced amount of work of MMSE-based schemes in MIMO and frequency selective channels. However, if the sparseness of the matrices is taken into account, only a fraction of the memory and computing power is required.

The Enhanced-MMSE (E-MMSE) receiver adds a PIC after the MMSE algorithm. The cancelling algorithm consists of removing the estimated interference from the matched filter result. The initial estimate is obtained from the MMSE result.

$$\mathbf{y}_1 = SDD(\mathbf{y}_{MMSE}, \sigma_{estim}^2)$$

where σ_{MMSE}^2 is the noise variance of \mathbf{y}_{MMSE} .

The cancellation operates on the MF result, and is simply the simultaneous removal of all influences that the symbols have on each other, throughout the transmission and receiver operations, in the absence of noise (accomplished with the removal of the main diagonal of \mathbf{R})

$$\mathbf{y}_{n+1} = \mathbf{y}_{MF} - (\mathbf{R} - \text{diag}(\mathbf{R})) \mathbf{y}_n$$

The result is then normalized and passed through the SDD, becoming the estimate for the next iteration

$$\mathbf{y}_{n+1} = SDD\left(\mathbf{y}_{n+1} \mathbf{e}_{NORM}, \sigma_{MMSE}^2\right)$$

where \mathbf{e} represents element-wise multiplication. The normalization consists simply of inverting the main diagonal of \mathbf{R} , $\mathbf{e}_{NORM} = \text{diag}(\mathbf{R})^{-1}$, so as to compensate for the spreading, amplitude, channel power and cross-correlation between symbols. The function $sdd()$ is the soft decision device function and $\text{diag}()$ refers to all the elements in the diagonal of a matrix. Note that the initial MMSE output does not need any normalization, since this is accomplished by the equalization from the \mathbf{E}_M .

The SDD is based on the assumption that the remaining noise in the estimates is essentially AWGN (Divsalar, 1998), being taken as optimum under this assumption. Taking x as either the real or imaginary component of the symbol, and considering that the real and imaginary part of the QPSK constellation both consist of $\{-1,1\}$, the SDD for the QPSK modulation is given by

$$y = \tanh\left(\frac{x}{\sigma_x^2}\right)$$

Applying the same reasoning for the 16QAM case (assuming that the real/imaginary constellation components point have values of $\{-3,-1,1,3\}$), we get

$$y = \frac{3e^{-\frac{4}{\sigma_x^2}} \sinh\left(\frac{3x}{\sigma_x^2}\right) + \sinh\left(\frac{x}{\sigma_x^2}\right)}{e^{-\frac{4}{\sigma_x^2}} \cosh\left(\frac{3x}{\sigma_x^2}\right) + \cosh\left(\frac{x}{\sigma_x^2}\right)}$$

where σ_x^2 is the noise power of each real/imaginary component of the symbol prior to SDD.

Figure 2 illustrates the PIC. The added complexity to the MMSE algorithm is negligible since the main system matrices (S, C, A, R) required by the PIC have already been computed for the MMSE operation. The iterative algorithm only needs to multiply the current estimated symbol by pre-defined matrices, while performing the SDD. The main difference from the PIC structure shown to conventional PIC schemes is the fact that this new scheme makes use of the MMSE's structure and thus is able to correctly estimate the interference caused by ISI (Inter-Symbolic Interference) and MAI (Multiple Access Interference), aside the thermal noise component. The used normalization factor is also improved since, besides containing the effect of spreading and channel power, it contains the cross-correlation effects caused by multipath, which in conventional receivers isn't used.

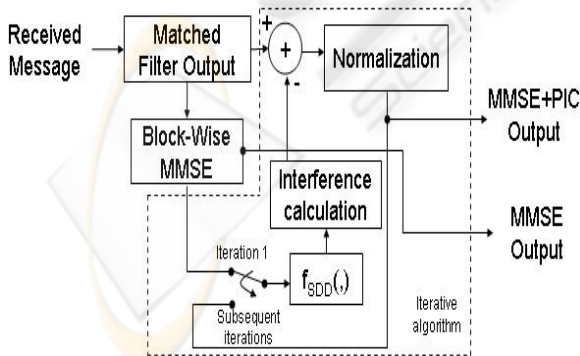


Figure 2 : PIC Structure

3 SIMULATION SETUP & RESULTS

This work was inspired on the uncoded 3G HSDPA standard, and thus considers a SF=16 using Hadamard codes, QPSK and 16QAM modulation, a chip rate of 3.84 Mcps and a Gold-sequence scrambling code. Each TX antenna can thus host a maximum of 16 physical channels. One user per physical channel is assumed. Simulations were run for SISO and MIMO orders 2 and 4, so that all the expected future UE types were covered. Minimum and full loading (0 and 15 interferers per transmit antenna respectively, assuming that the main user is using the first physical channel of each antenna) was considered. The E-MMSE scheme used cancellation of two iterations after the MMSE decoding. Blocks of 1024 bits per physical channel per antenna were used.

The main UMTS channels, namely Indoor A, Pedestrian A and Vehicular A (taken from (3GPP TR 25.943)) were simulated. Since only 1 sample per chip was used in the simulations, the channels were adjusted to the chip delay time of 260ns, using the constant mean delay spread method (Silva, 2003). For the particular case of Vehicular A, since the method yields 8 taps, with the last ones having low power levels, an adjustment was made so that only the main taps were considered. The resulting channels are depicted in Figure 3. The considered velocities were 50km/h for Vehicular A and 3km/h for the remaining channels.

IndA	delay (chips)	0	1		
	% received power	90,63%	9,37%		
PedA	delay (chips)	0	1		
	% received power	94,98%	5,02%		
VehA	delay (chips)	0	1	3	4
	% received power	49,50%	39,32%	6,23%	4,95%

Figure 3 : Resulting UMTS channels

The Monte Carlo method was employed for the simulations. All results were portrayed for received E_b/N_0 values vs BER (Bit Error Rate). For the sake of comparison, we also considered the simple MMSE receiver.

Based on the results of figure 4, only two PIC iterations are needed to achieve the best results; all results in the posterior figures thus consider only two iterations for the E-MMSE scheme.

In figures 5-8, the E-MMSE results for different MIMO orders, channels, modulations and loadings can be observed. The performance curves are parallel to the MMSE results, though a little deviated to the left; i.e. there is an offset of the curves corresponding to the performance gain over MMSE. Figures 9-11

compare some of the results of the E-MMSE to the simple MMSE algorithm.

For the SISO case without interference, there is a negligible difference between the E-MMSE and MMSE. This was expected, since the canceller is only rearranging the results so that the estimates symbols do not exceed their thresholds. For the MIMO 2x2 case without interference, differences between 1dB and 2dB can be found between channels and modulations, with the biggest differences being registered for QPSK modulations (due to smaller probabilities of bit errors, and thus having a very small error propagation in the canceling algorithm).

In the full loading scenario (15 interferers), differences over 5dB and 3dB can be found for QPSK and 16QAM respectively. The differences are greater than for the case of minimum loading, due to the PIC canceling interference from other users, thus being more effective.

3.1 E-MMSE Results

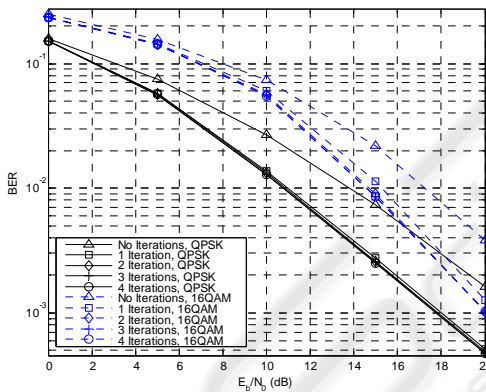


Figure 4 : BER performance for E-MMSE, Vehicular A channel, MIMO 2x2, 15 interferers - effect on number of cancelling stages.

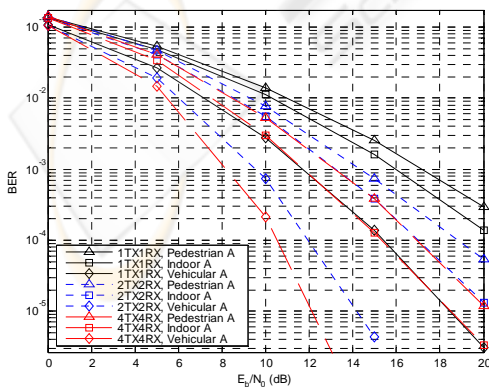


Figure 5 : E-MMSE scheme – QPSK modulation, 0 interferers

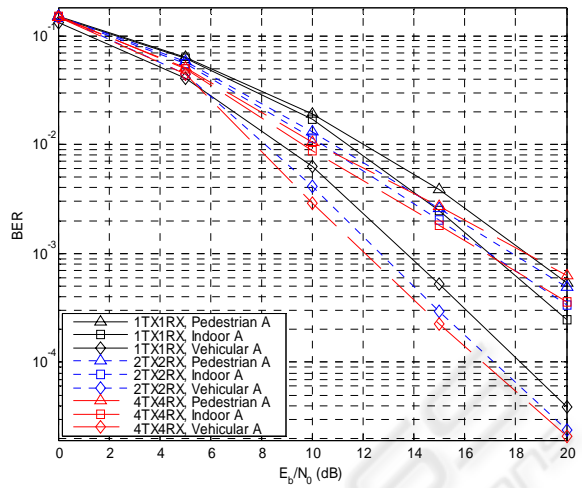


Figure 6 : E-MMSE scheme – QPSK modulation, 15 interferers

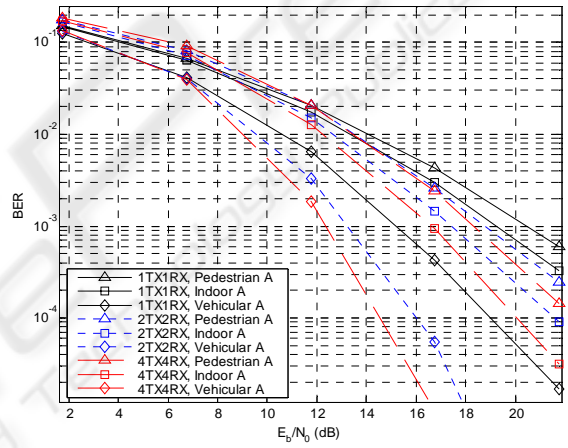


Figure 7 : E-MMSE scheme – 16QAM modulation, 0 interferers

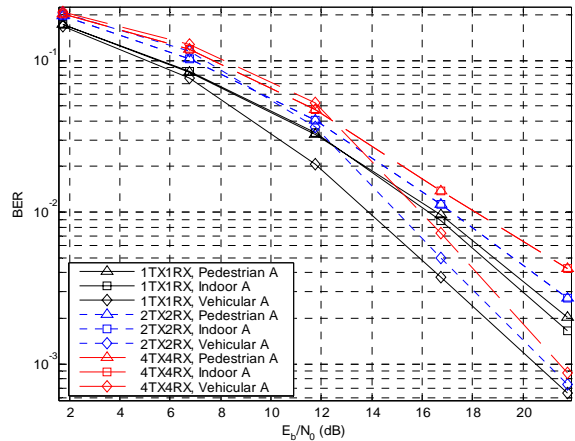


Figure 8 : E-MMSE scheme – 16QAM modulation, 15 interferers

3.2 E-MMSE vs MMSE Comparison

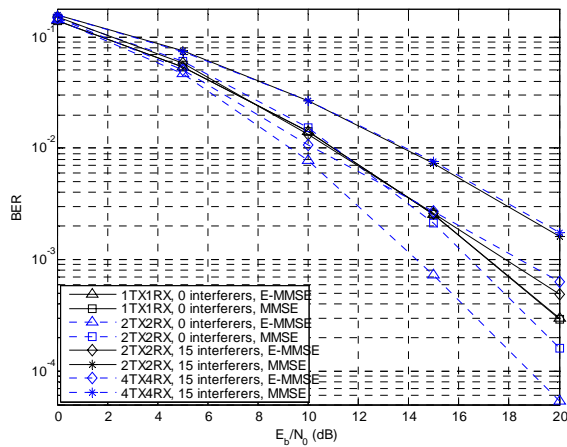


Figure 9 : E-MMSE vs MMSE scheme – QPSK modulation, Pedestrian A channel

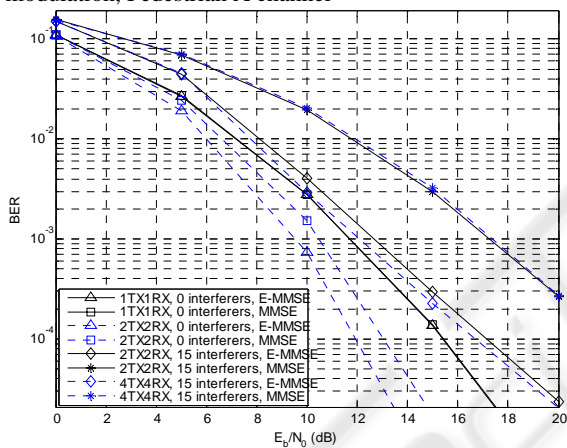


Figure 10 : E-MMSE vs MMSE scheme – QPSK modulation, Vehicular A channel

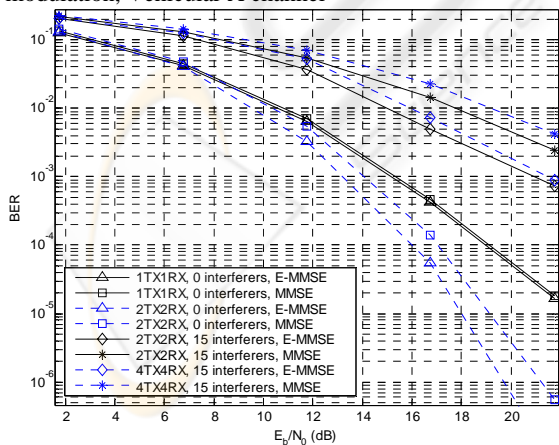


Figure 11 : E-MMSE vs MMSE scheme – 16QAM modulation, Vehicular A channel

4 CONCLUSIONS

In this work, an iterative PIC was added to a MIMO-BLAST MMSE receiver considering frequency-selective fading channels, using the same structure as that required by the MMSE. The used PIC is able to cancel out most of the interference caused by multipath, cross-correlation between users/antennas and thermal noise. It was shown that with a small increase in complexity, gains over 5dB and 3dB can be achieved for QPSK and 16QAM respectively, in what is considered one of the best joint-detection receiver algorithms presently.

ACKNOWLEDGEMENTS

This paper was elaborated within the B-BONE (Broadcasting and Multicasting over Enhanced UMTS Mobile Broadband Networks) project, and was partially funded by the Foundation of Science and Technology (FCT), of the Portuguese Ministry of Education.

REFERENCES

G. J. Foschini and M. J. Gans, "On limits of wireless communications in a fading environment when using multiple antennas," *Wireless Pers. Commun.*, vol. 6, pp. 311–335, Mar. 1998.

M. Latva-aho, M. Juntti, "LMMSE Detection for DS-CDMA Systems in Fading Channels", *IEEE Transactions on Communications*, vol.48, no2, February 2000.

George, Alan and Joseph Liu, *Computer Solution of Large Sparse Positive Definite Systems*, Prentice-Hall, 1981.

D. Divsalar, M. Simon and D. Raphaeli, "Improved Parallel Interference Cancellation in CDMA", *IEEE Trans. Commun.* Vol.46, pp.258-268, February 1998.

3GPP, *Deployment aspects*, 3GPP TR 25.943 v5.1.0, Sophia Antipolis, France, 2002.

J. C. Silva, N. Souto, A. Rodrigues, F. Cercas and A. Correia, "Conversion of reference tapped delay line channel models to discrete time channel models", *VTC03 Fall*, Orlando, Florida, 6-9 Oct. 2003.